Am J Cancer Res 2022;12(6):2697-2710
www.ajcr.us /ISSN:2156-6976/ajcr0142380

Original Article

Eltrombopag binds SDC4 directly and enhances MAPK signaling and macropinocytosis in cancer cells

Can Cui[1,2*], Yuting Pan[1,2*], Chengqian Zhang[3*], Darong Zhu[1,2], Ying Xuan[1,2], Piliang Hao[3], Xisong Ke[1,2], Xianglian Zhou[1,2], Yi Qu[1,2]

[1]Center for Chemical Biology, Institute of Interdisciplinary Integrative Medicine Research, Shanghai University of Traditional Chinese Medicine, Shanghai, China; [2]Shanghai Frontiers Science Center of TCM Chemical Biology, Institute of Interdisciplinary Integrative Medicine Research, Shanghai University of Traditional Chinese Medicine, Shanghai, China; [3]School of Life Science and Technology, ShanghaiTech University, Shanghai, China. [*]Equal contributors.

Received February 16, 2022; Accepted May 7, 2022; Epub June 15, 2022; Published June 30, 2022

Abstract: Syndecan-4 (SDC4) is a single-pass transmembrane glycoprotein implicated in a variety of oncogenic signaling pathways. It is also an intrinsically disordered protein and considered "undruggable". In the present study, we confirmed that knocking out SDC4 in pancreatic cancer cells markedly impaired macropinocytosis, colony formation, as well as xenograft tumor initiation and growth. Quantitative proteomic profiling of Sdc4 knockout (KO) cells revealed significant changes in cell metabolic pathways. In a cellular protein-based ligand interaction screening, we identified that Eltrombopag (ETBP), an FDA-approved agonist of the thrombopoietin receptor (TPOR) for immune thrombocytopenia, could directly bind to SDC4 with a Kd value of ~2 μM. We showed that the transmembrane motif was essential for SDC4 binding to ETBP. Unexpectedly, ETBP not only increased SDC4 abundance, but also enhanced SDC4-associated MAPK signaling pathway and macropinocytosis in cancer cells. Our results indicate that ETBP is a potential agonist of SDC4 in a fashion similar to its original target TPOR, and that caution should be taken when using ETBP for chemotherapy-induced thrombocytopenia in cancer patients.

Keywords: Syndecan-4, eltrombopag, MAPK signaling pathway, macropinocytosis, cancer

Introduction

Syndecans (SDCs) are a family of transmembrane proteoglycans implicated in various physiological processes [1, 2]. In vertebrates, four types of syndecans (SDC1-4) are expressed throughout the body [3]. They have been closely linked to the occurrence and progression of breast [4], prostate [5], colon [6], and pancreatic cancers [7]. SDC4 is an important member of the SDC family and positively associated with different tumor types and oncogenic processes such as cell proliferation, invasion, and migration [8-11]. In addition, SDC4 also functions as a co-receptor of the fibroblast growth factor receptor (FGFR) and enhances the mitogen-activated protein kinase (MAPK) signaling pathway [12]. However, validation of SDC4's roles in cancer remains lacking, especially via loss-of-function assays.

SDC4 mainly consists of three domains, the N-terminal ectodomain attached to glycosaminoglycans, a single transmembrane motif essential for dimerization, and the C-terminal cytoplasmic domain where constant regions (C1 and C2) flank a variable region (V) that is unique to each syndecan [3, 13]. In some cases, syndecans may be cleaved near the membrane by matrix metalloproteinases (MMPs) [14-16], a process known as shedding [17]. The shed syndecan ectodomains are soluble and capable of binding to components of the extracellular matrix (ECM), growth factor receptors, and integrins [18, 19]. Notably, there are no experimental 3D structures of full-length SDC4 [3], likely due to nearly 55% of its amino acid residues belonging to the intrinsically disordered protein region (IDPR) [20, 21]. SDC4 is thus considered a typical "undruggable" protein [22].

The small-molecule drug eltrombopag (ETBP) has been previously identified as a non-peptide agonist of the thrombopoietin receptor (TPOR) [23]. ETBP activates TPOR-specific signal trans-

duction, and cell proliferation and differentiation via activating STAT5, mitogen-activated protein kinase, P38, and other early response genes [23]. Since its approval in 2008, ETBP has been used worldwide for treating immune thrombocytopenia (ITP) [24, 25]. Additionally, ETBP has been approved to treat severe aplastic anemia in combination with immunosuppression in Europe and United States [26]. Moreover, ETBP has also proven effective for treating diseases such as chemotherapy-induced thrombocytopenia (CIP) [27], selected inherited thrombocytopenias [28], and myelodysplastic syndromes [29, 30]. In the present study, we demonstrate that ETBP can directly bind to SDC4 and enhance SDC4-associated oncogenic activities in tumor cells. Our findings support ETBP as a potential SDC4 activator and underline the potential complications that may result from the clinical use of ETBP for CIP in cancer patients.

Materials and methods

Chemicals

Eltrombopag (SB-497115) was purchased from SelleckChem (Shanghai, China). The FDA-approved drug library (L1021) was purchased from APExBIO (Shanghai, China).

Cell culture

Pancreatic cancer cell lines AsPC1 (TCHu8), BxPC3 (TCHu12), CFPAC1 (TCHu112), and PANC1 (TCHu98) and the colon cancer cell line HCT116 (TCHu99) were purchased from the National Collection of Authenticated Cell Cultures (Shanghai, China). AsPC1 and BxPC3 cells were cultured in RPMI 1640 medium (Thermo Fisher Scientific) and PANC1 cells were cultured in DMEM medium (Thermo Fisher Scientific). The medium was supplemented with 10% fetal bovine serum (FBS) (Gibco, Gaithersburg, MD) and 1% penicillin-streptomycin (Hyclone, Logan, UT). All cell lines were maintained at 37°C in a humidified atmosphere consisting of 5% CO_2.

Generation of SDC4 KO cells through CRISPR/Cas9-mediated gene editing

The *SDC4* gene was deleted in PANC1 and HCT116 cells by CRISPR/Cas9 genome editing. A plasmid pL-CRISPR.EFS.GFP (#57818, Addgene) encoding both the Cas9 protein and the sgRNA was used. The Cas9 sequence is coupled to a P2A site and EGFP. Expression of the Cas9 protein results in simultaneous expression of EGFP, allowing for the selection of positively transfected cells. Two sgRNAs targeting exon4 and exon5 of the *SDC4* gene were designed using the optimized CRISPR design online tool (http://crispr.cos.uni-heidelberg.de). The oligo sequences for the sgRNAs are listed below: sgRNA1 for exon4 forward, 5'-CACCGCACCGAACCCAAGAAACTAG-3', reverse, 5'-AAACCTAGTTTCTTGGGTTCG-GTGC-3'; sgRNA2 for exon5 forward, 5'-CACCGTCTCTGCCTGGGCAAGAGTG-3', reverse, 5'-AAACCACTCTTGCCCAGGCAGAGAC-3'. Plasmids were then sequenced by Sangon Biotech Company (Shanghai, China) to check the right insertion. Two CRISPR/Cas9 plasmids were co-transfected in equimolar ratio into cells using Lipofectamine3000 (L3000075, Invitrogen). After transfection for 48 h, EGFP-positive single cells were sorted into 96-well plates and the plates were kept in the incubator for 7-14 days. Genomic DNA was extracted with QuickExtract DNA Extraction Solution (QE09050, Epicenter, Madison, WI) for PCR identification followed by Sanger-sequencing. The sequences of PCR primers are shown as below: forward, 5'-GCAGCATAATTGTGGAGA-3'; reverse, 5'-CTGTGGAAATGTGCGAGA-3'.

Western blot analysis

Cells were lysed using RIPA (#9806, Cell Signaling Technology) containing protease inhibitors (#36978, Thermo Fisher Scientific) at 4°C and proteins were quantified by the BCA protein quantification kit (#23227, Thermo Fisher Scientific). Proteins (10-30 μg per lane) were separated by SDS-PAGE and then transferred onto polyvinylidene fluoride membranes (#P0807, Millipore). Subsequently, the membranes were blocked with 5% non-fat milk for an hour before incubation with primary antibodies overnight at 4°C. The antibody against SDC4 (NB110-41551) was purchased from Novus, Antibodies against SDC1 (12922), p-ERK (4370S), ERK (4695S), p-AKT (4060S), AKT (9272S), p-P38 (4511S), P38 (8690S), and GAPDH (D16H11) were purchased from Cell Signaling Technology. Finally, the membranes were incubated with HRP-goat anti-rabbit secondary antibodies (1:10000, 7074S, CST) for 1 hour. Enhanced chemiluminescence

detection reagent (#P10300, NCM Biotech) was used to visualize the signal strength of the bands.

Macropinocytosis

The macropinocytic index was determined according to the protocol previously described [47]. Briefly, cells were seeded into 48-well plates (Costar) for 24 hours, before being serum-starved for 12 hours and subsequent incubation with 1 mg/ml TMR-dextran (#T11-62, Sigma) for 35 minutes at 37°C. At the end of the incubation period, cells were rinsed five times in cold PBS and immediately fixed in 4% polyformaldehyde solution for 15 minutes. Cells were mounted with 0.1 mg/ml DAPI (#C1002, Beyotime) for nuclear staining. Images were captured with an ImageXpress Micro 4 microscope (Molecular Devices) using standard settings. Mean fluorescence intensity was determined by calculating the integrated signals from at least 10 fields that were randomly selected from different regions across the entirety of each sample.

Quantitative RT-PCR (qRT-PCR)

Total RNA was extracted with TRIzol (T9424, Sigma) according to the manufacturer's instructions. The reverse transcription reaction was performed with the 5x *Evo M-MLV*RT Master Mix (AG11706, Accurate Biology). Expression of the indicated genes was assessed with the QuantStudio5 real-time PCR instrument (Applied Biosystems) using the Hieff qPCR SYBR Green Master Mix (Low Rox Plus) kit (11202ES03, Yeasen). Reaction plates were incubated in a 384-well thermal cycling plate at 95°C for 10 min and then underwent 40 cycles of 10 s at 95°C and 30 s at 60°C. All reactions were performed in triplicates. Relative quantitation was calculated using the $2^{-\Delta Ct}$ method, where ΔCt symbolizes the change in Ct between the sample and reference mRNA. The ologo sequences for PCR primers are: *SDC4*, 5'-GGCAGCTCTGATTGTGGGT-3' (forward), 5'-CATACGGTACATGAGCAGTAGGA-3' (reverse); *GAPDH*, 5'-ACAACTTTGGTATCGTGGAAGG-3' (forward), 5'-GCCATCACGCCACAGTTTC-3' (reverse).

Flow cytometry

Cells were resuspended in the Non-enzymatic Cell Dissociation Buffer (C5789, Sigma). The cell pellet was then resuspended in cold PBS with 1% (w/v) BSA. To measure surface populations of SDC4, resuspended cells (>10,000) were incubated with FITC-conjugated anti-SDC4 or its isotype-matched control antibody (sc-12766, Santa Cruz) for 15 minutes on ice and processed for flow cytometry analysis following the manufacturer's instructions. To measure total SDC1, resuspended cells were immediately fixed in PBS containing 1.6% polyformaldehyde and permeabilized in 0.5% saponin before incubation with conjugated antibodies. Flow Cytometry (CytoFLEX S, Beckman) data were analyzed using the CytExpert software according to the manufacturer's specifications. SDC4 protein expression data were obtained from two independent experiments.

Protein preparation and mass spectrometry analysis

Cell lysate was sonicated and centrifuged to pellet cellular debris. Lysate protein concentrations for all samples were determined by the Pierce BCA Assay (Thermo Fisher Scientific, Franklin, Massachusetts) per the manufacturer's instructions. Total protein was reduced with 10 mM 1,4-dithiothreitol (DTT) at 37°C for 1 h and subsequently alkylated in 20 mM iodoacetamide (IAA) for 30 min at room temperature in the dark. Proteins were digested with trypsin (1:50, w/w) at 37°C overnight. All the tryptic peptides in the samples were desalted on a Sep-pak C18 cartridge column and then lyophilized under vacuum.

The vacuum-dried samples were resuspended in 0.1% FA for liquid chromatography (LC)-MS/MS analysis. Each sample of peptides was loaded onto a C18 trap column (75 μm ID×2 cm, 3 μm, Thermo Scientific) and then separated on a C18 analytical column (75 μm ID×50 cm, 2 μm, Thermo Scientific). Peptides were separated and analyzed on an Easy-nLC 1200 system coupled to a Q-Exactive HF-X Hybrid Quadrupole-Orbirap Mass spectrometer system (Thermo Fisher Scientific). Mobile phase A (0.1% formic acid in 2% ACN) and mobile phase B (0.1% formic acid in 98% ACN) were used to establish a 120 min gradient composed of 1 min of 5% B, 106 min of 5-28% B, 2 min of 28-38% B, 1 min 38-90% B, 10 min of 90% B at a constant flow rate of 250 nL/min at 55°C. MS data were acquired with the instrument operating in the data dependent mode.

Peptides were then ionized by electrospray at 2.2 kV. Full-scan MS spectra (from m/z 375 to 1500) were acquired in the Orbitrap at a high resolution of 120,000 with an automatic gain control (AGC) of 3×10^6 and a maximum fill time of 20 ms. The twenty most intense ions were sequentially isolated and fragmented in the HCD collision cell with normalized collision energy of 27%. Fragmentation spectra were acquired in the Orbitrap analyzer with a resolution of 15,000. Ions selected for MS/MS were dynamically excluded for a duration of 30 s.

The raw data were processed using MaxQuant with the integrated Andromeda search engine (v.1.5.4.1) against the human protein database (release 2016_07, 70630 sequences) with a common contaminant database (215 entries). Enzyme was set to trypsin allowing N-terminal cleavage to proline and two missed cleavages were allowed. Database searches were performed with the following parameters: precursor mass tolerance was up to 10 ppm and the product ion mass was up to 0.02 Da. Cysteine carbamidomethylation was set as a fixed modification and N-terminal acetylation, oxidation (M), and deamidation (NQ) were set as variable modifications. A false discovery rate (FDR) of 0.01 was required for proteins and peptides.

Microscale thermophoresis (MST)

Ten million HEK293T cells overexpressing EGFP alone or EGFP-tagged SDC1, SDC2, SDC3, or SDC4 were lysed in 0.5 mL RIPA (#9806, Cell Signaling Technology) containing protease inhibitors (#36978, Thermo Fisher Scientific). Cell lysates were diluted in PBS buffer to a final concentration at which EGFP fluorescence signals were suitable for detection on the Monolith NT.115 instrument (NanoTemper Technologies). A collection of 1,363 FDA-approved drugs was used for binding check screening. For binding affinity detection, a 10 μL protein sample was mixed with a 10 μL ligand solution at the appropriate concentrations. The purified proteins were labeled by the Red-NHS kit following the manufacturer's protocol (MO-L011, NanoTemper Technologies). Then the mixture solutions were loaded into NT.115 standard coated capillaries or premium coated capillaries (NanoTemper Technologies). MST measurements were performed at 25°C. The fluorescence signal during thermophoresis was monitored and the change in fluorescence was analyzed by the software. Kd values were calculated by fitting a standard binding curve to the series of diluted ligands.

Recombinant protein purification

The cDNA encoding human SDC4 (P31431) was synthesized (Genscript, China) and cloned into pGEX-6P-1 to enable N-terminal glutathione S-transferase (GST)-tagging of the SDC4 protein. The construct was transformed into the expression host *E. coli* stain BL21 (DE3) and the cells were grown in YEP medium at 37°C until OD_{600} of 0.6. The cells were then induced by adding 0.1 mM isopropyl-β-D-l-thiogalactopyranoside (IPTG) to the culture and grown at 18°C overnight. Cells were harvested by centrifugation. The cell pellet was resuspended in a buffer containing 20 mM Tris (pH 7.5), 500 mM NaCl, and 2 mM DTT and lysed by sonication. After centrifugation, the clarified cell lysate was incubated with glutathione-sepharose 4B beads. GST-tagged SDC4 was eluted with the buffer consisting of 50 mM reduced glutathione. Protein fractions were collected in buffer containing 20 mM Tris (pH 7.5), 150 mM NaCl, and 2 mM DTT and used for the indicated assays.

CCK-8 assays

The CCK-8 (Cell-Counting Kit-8) assay was used to detect the cell proliferation and ligand cytotoxicity following the manufacturer's protocol (APExBIO). Cells were seeded into 96-well plates at a density of 5,000 cells/well overnight at 37°C. The cells were then treated with different concentrations of ligands for 24 hours and 72 hours, respectively. Then 10 μL CCK-8 reagent was added into each well and incubated for another 2 hours, OD_{450} was measured by a microplate reader (Spark, TECAN).

Colony formation assays

Colony formation assays were performed according to the protocol described previously [48]. Briefly, ~200 single cells were seeded into each well in a 6-well plate. Medium was changed every 3 days for 2 weeks. Colonies that formed were fixed with PBS containing 4% formaldehyde and stained with 0.005% crystal violet.

Xenograft tumor assays

Male BALB/c nude mice (four weeks old) were purchased from Sino-British SIPPR/B&K Lab Animal Ltd (Shanghai, China) and housed under pathogen-free conditions. PANC1-SDC4-WT or PANC1-SDC4-KO cells (1×10^7) were injected subcutaneously into the left flank of nude mice. Tumors were measured with a caliper and volume was calculated using the formula V = (width^2 × length)/2. Mice were sacrificed when tumor volumes reached 300 mm^3.

Statistical analysis

The results were expressed as mean ± SD. Data analysis was performed using GraphPad Prism version 7.

Results

Establishing SDC4 knockout (KO) cancer cells

SDC4 abnormal expression has been previously linked to tumor progression and poor prognosis in various malignant tumors [8, 31-33]. Here, we further evaluated SDC4 expression using the Cancer Genome Atlas (TCGA) dataset. The results indicated that SDC4 was clearly highly expressed in pancreatic adenocarcinoma (PAAD) and colon adenocarcinoma (COAD) compared to normal tissues (**Figure 1A**, **1B**). High SDC4 expression was also significantly associated with shorter overall survival (OS) of PAAD patients (**Figure 1C**, **1D**), suggesting that SDC4 is a potential positive regulator of PAAD and COAD.

To validate our TCGA data and determine whether SDC4 is required for tumor progression, we knocked out SDC4 in cancer cells via the CRISPR-Cas9 gene-editing technology (**Figure 1E**). The sgRNAs were designed to target the cytoplasmic domain that is important for intracellular signal transduction (**Figure 1E**). We obtained two SDC4 KO pancreatic PANC1 cell clones and one SDC4 KO colorectal HCT116 cell clone. Genomic DNA sequencing confirmed the deletion of exon4 and exon5 in the SDC4 locus (**Figure 1F**). SDC4 KO was further confirmed by RT-PCR assays of SDC4 mRNA expression (**Figure 1G**, **1H**), and western blotting (**Figure 1I**, **1J**) and flow cytometry analysis of SDC4 proteins (Figure S1C). Notably, the expression level of SDC1 protein was almost unchanged in SDC4 KO cells (**Figure 1I**, **1J**), supporting the specificity of the SDC4-targeting sgRNAs. Of note, the molecular weights of SDC4 and SDC1 were lower than expected in western blotting assays (Figure S1), indicating that SDC4 could be cleaved in the cells tested as described in previous studies [34-36].

SDC4 is required for tumor initiation and growth

SDC4 KO cells exhibited no significant differences in culture, both in their epithelial morphology and growth rates (Figure S2A, S2B). To determine whether SDC4 is required for tumorigenic activity, we performed colony-forming assays and found that SDC4 KO markedly impaired the colony-forming ability of PANC1 cells (**Figure 2A**), while no difference was detected in SDC4 KO HCT116 cells (**Figure 2E**). Furthermore, SDC4 KO markedly inhibited the growth of both PANC1 and HCT116 xenograft tumors (**Figure 2B**, **2C**, **2F**, **2G**). Notably, SDC4 KO also significantly decreased the ability of tumor initiation (**Figure 2D**, **2H**).

SDC1 has been reported to be a critical mediator of macropinocytosis, a regulated form of endocytosis for nutrient salvage to sustain uncontrolled growth [7]. And SDC4 overexpression cells exhibit a two-fold increase in peptide internalization [37]. To investigate whether SDC4 is also associated with macropinocytosis in PDAC cells, we performed the tetramethylrhodamine-labeled dextran (TMR-dextran) uptake assay in SDC4 KO PANC1 cells, and detected a clear decrease (~50%) of macropinocytosis compared with wide-type PANC1 cells (**Figure 2I**, **2J**). Decreased macropinocytosis was also observed in SDC4 KO HCT116 cells (Figure S2C, S2D). Collectively, these findings confirm the importance of SDC4 in tumor progression.

SDC4 is associated with cell metabolism

Although SDC4 has been implicated in various signaling pathways [38], loss-of-function studies that validate such roles of SDC4 remain lacking. Taking advantage of the SDC4 KO cells, we next performed proteomic profiling analysis of wide-type and SDC4 KO PANC1 cells. A total of 6,201 proteins were detected among three cell lines with two repeat experi-

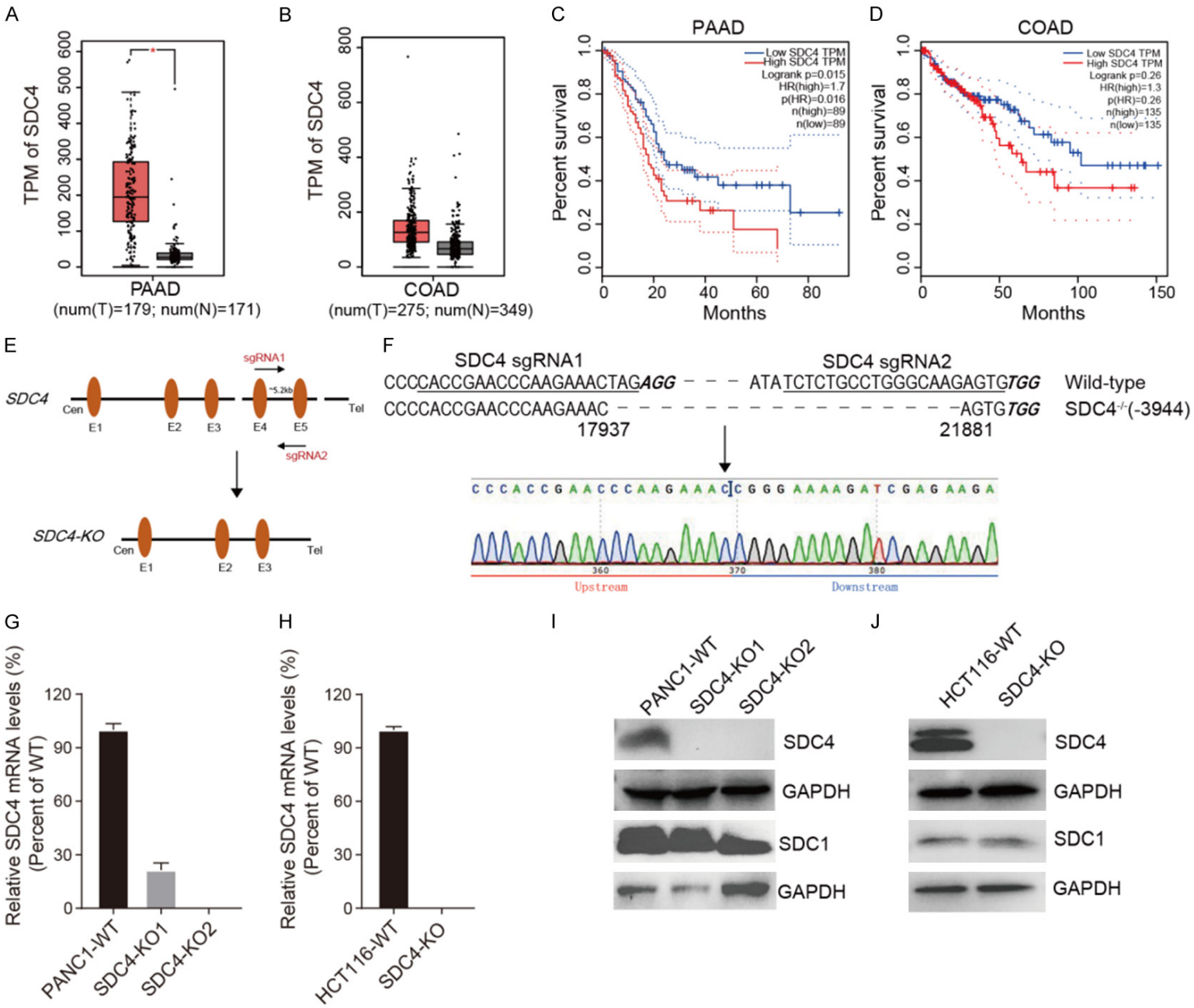
A
TPM of SDC4
PAAD
(num(T)=179; num(N)=171)
B
TPM of SDC4
COAD
(num(T)=275; num(N)=349)
C
PAAD
Low SDC4 TPM
High SDC4 TPM
Logrank p=0.015
HR(high)=1.7
p(HR)=0.016
n(high)=89
n(low)=89
Percent survival
Months
D
COAD
Low SDC4 TPM
High SDC4 TPM
Logrank p=0.26
HR(high)=1.3
p(HR)=0.26
n(high)=135
n(low)=135
Percent survival
Months
E
SDC4
sgRNA1
sgRNA2
Cen
Tel
E1
E2
E3
E4
E5
SDC4-KO
F
SDC4 sgRNA1
SDC4 sgRNA2
CCCCACCGAACCCAAGAAACTAGAGG - - - ATATCTCTGCCTGGGCAAGAGTGTGG Wild-type
CCCCACCGAACCCAAGAAAC - - - - - - - - - - - - - - - - AGTGTGG SDC4-/-(-3944)
17937
21881
Upstream
Downstream
G
Relative SDC4 mRNA levels (%)
(Percent of WT)
PANC1-WT
SDC4-KO1
SDC4-KO2
H
Relative SDC4 mRNA levels (%)
(Percent of WT)
HCT116-WT
SDC4-KO
I
PANC1-WT
SDC4-KO1
SDC4-KO2
SDC4
GAPDH
SDC1
GAPDH
J
HCT116-WT
SDC4-KO
SDC4
GAPDH
SDC1
GAPDH

Figure 1. CRISPR/Cas9 KO of SDC4 in cancer cells. (A, B) TCGA data analysis of SDC4 gene expression in pancreatic adenocarcinoma (A) and Colon adenocarcinoma (B) against normal tissues (http://gepia.cancer-pku.cn). *P<0.05. (C, D) Survival analysis and correlation with SDC4 expression in pancreatic adenocarcinoma (C) and colon adenocarcinoma (D) in TCGA dataset (n=89). The median overall survival value was used. (E) Schematic diagram of CRISPR/Cas9 KO of SDC4. (F) Location and sequences of the SDC4-targeting sgRNAs. (G, H) Quantitative RT-PCR assays of SDC4 deletion in PANC1 (G) and HCT116 (H) cells. (I, J) Western blot assays of SDC4 deletion in PANC1 (I) and HCT116 (J) cells.

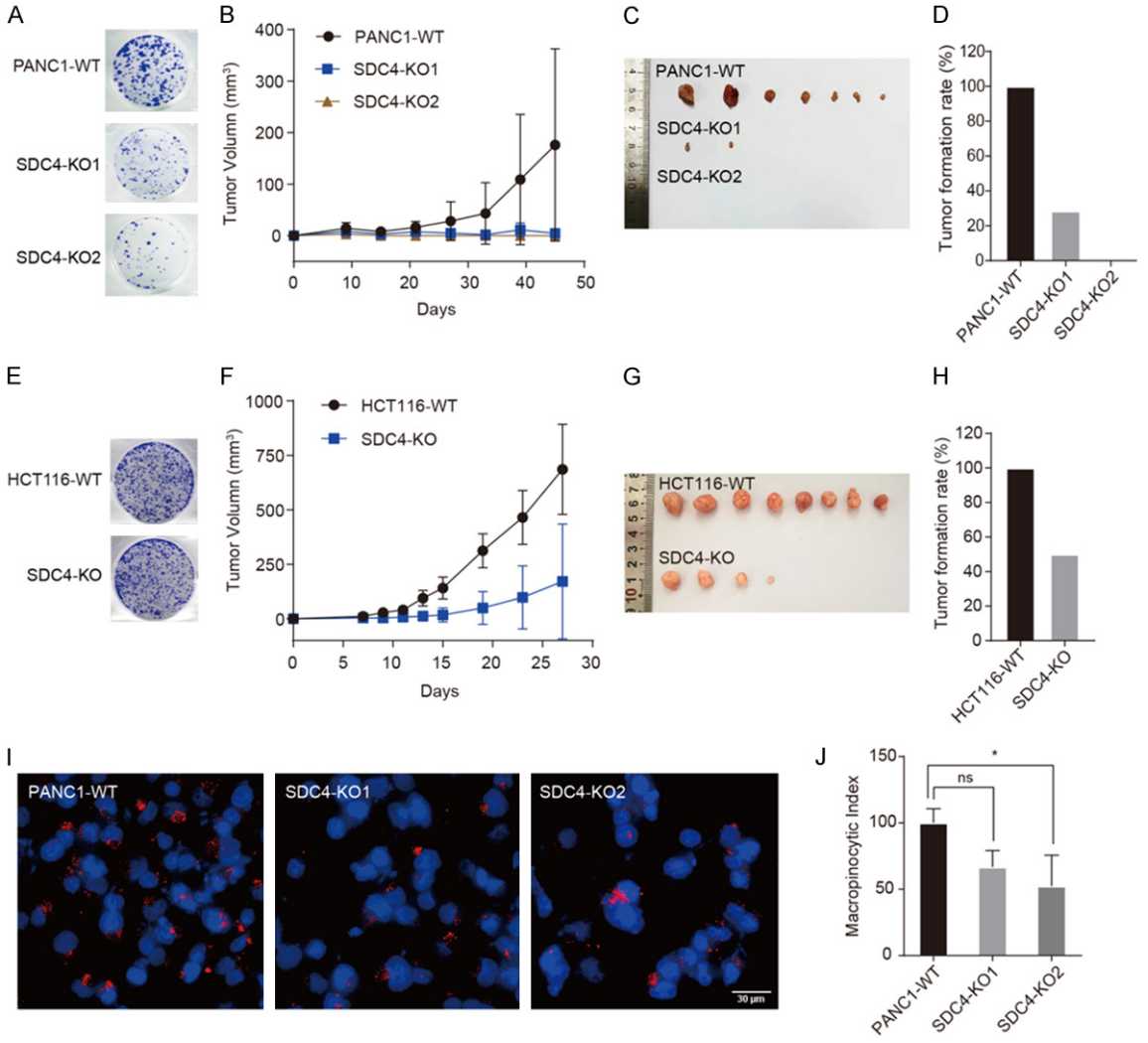

Figure 2. Phenotypic characterization of SDC4 KO cancer cells. (A) Representative images of the clonogenic assay for wild-type and SDC4 KO PANC1 cells. Experiments were repeated twice with similar results. (B, C) Xenograft tumor assays of SDC4 KO PANC1 cells. The tumor growth curve (B) and the image of the tumor at the conclusion of the experiment (C) are presented. (D) The tumor initiation rate of SDC4 KO PANC1 cells. (E) Representative images of the clonogenic assay for wild-type and SDC4 KO HCT116 cells. (F, G) Xenograft tumor assays of SDC4 KO HCT116 cells. The tumor growth curve (F) and the image of tumors at the conclusion of the experiment (G) are presented. (H) The tumor initiation rate of SDC4 KO HCT116 cells. (I, J) TMR-dextran visualization (I) and quantification (J) of macropinocytosis in wide-type and SDC4 KO PANC1 cells. Data are presented as mean ± SD. Scale bar, 30 μm.

ments. To identify significantly changed proteins, we performed a Student's t-test and used the threshold of >1.5 fold change to filter proteins. A total of 249 and 320 differentially expressed proteins were identified in SDC4-KO1 and SDC4-KO2 cells, respectively. Specifically, 89 proteins are shared by both SDC4 KO cell clones (**Figure 3A**; Table S1).

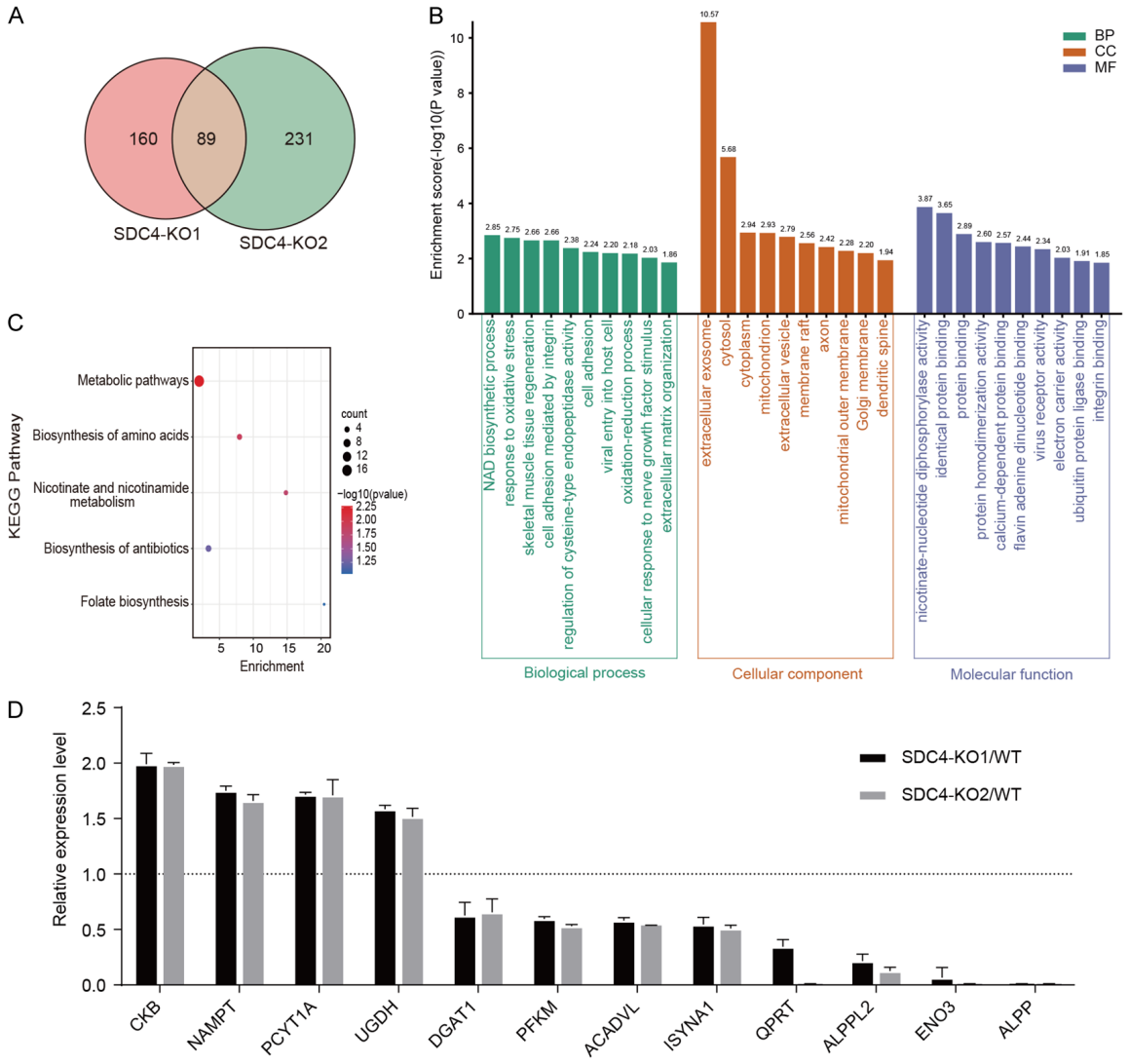

Figure 3. Proteomic profiling of proteins with altered expression in SDC4 KO PANC1 cells. A. A Venn diagram for changed proteins in the two SDC4 KO cell clones. The overlapping area indicates the shared 89 proteins. B. Top 10 Gene Ontology (GO) terms enriched in target proteins. C. Significantly enriched Kyoto Encyclopedia of Genes and Genomes (KEGG) pathways of the target proteins. D. Top 12 altered proteins involved in the metabolic pathways based on KEGG enrichment analysis.

To investigate the signature of the changed proteins, we performed gene ontology (GO) and Kyoto Encyclopedia of Genes and Genomes (KEGG) pathway enrichment analysis (**Figure 3B**, **3C**). According the top 10 GO terms, most of the changed proteins are involved in biological processes including NAD biosynthetic process, oxidative stress, cell adhesion, and viral entry (**Figure 3B**). The major cellular localizations of these proteins are extracellular exosome, cytosol, and membrane raft (**Figure 3B**). Functionally, these proteins have various activities, such as nicotinate nucleotide diphosphorylase activity, protein binding, and virus receptor activity (**Figure 3B**). The most enriched KEGG pathways are metabolic pathways, biosynthesis of amino acids, and nicotinate and nicotinamide metabolism, indicating that SDC4 mainly affects cellular metabolic pathways (**Figure 3C**). This is supported by the finding that the top 12 altered proteins are all involved in the metabolic pathway essential for cell energy and material metabolism (**Figure 3D**). Taken together, our proteomic profiling data indicate a strong association of SDC4 with metabolism.

ETBP directly targets SDC4 at the transmembrane motif

Given that SDC4 is an intrinsically disordered protein, conventional structure-based rational design is not suitable for identifying SDC4-targeting small molecules [21, 22]. To this end, we took advantage of the microscale thermophoresis (MST) assay that enables the examination of direct engagement between small molecules and cellular target proteins in biological liquids [39]. We thus prepared cell lysates from HEK293T cells expressing GFP-tagged SDC4 for single-point binding-check screening (**Figure 4A**). Within an FDA-approved drug library, ETBP was the compound with the biggest response (R) value (**Figure 4A**). Notably, ETBP was originally identified as an agonist of the transmembrane protein thrombopoietin receptor (TPOR) [23]. Direct engagment of ETBP with SDC4 was confirmed by the serial dilution MST assays where a Kd value of 2.2 μM was obtained (**Figure 4B**). To further verify the direct interaction, we purified GST-tagged recombinant SDC4 proteins. We were able to reproduce the MST binding curve and obtain the Kd value of 1.3 μM for ETBP binding to GST-SDC4 (**Figure 4C**). In this experiment, no significant binding curves were detected between ETBP and the GST protein (**Figure 4C**).

To investigate whether ETBP could bind to other syndecan proteins, we prepared lysates from cells expressing GFP-tagged SDC1, SDC2, and SDC3, respectively. Interestingly, direct binding was only observed between ETBP and SDC1 with a Kd value of 8.87 μM (**Figure 4D**), indicating relative selectivity of ETBP towards syndecan proteins. To determine the ETBP binding site, we constructed a series of GFP-tagged SDC4 truncation mutants (**Figure 4E**), whose expression was confirmed by western blotting (Figure S3). In cellular MST assays, all truncation mutants were able to engage with ETBP where Kd values ranged from 2 μM to 6.2 μM, except for M3 and M4 that contain a common depletion of the TM motif (**Figure 4F**, **4G**). These data indicate that the TM motif is essential for ETBP engagement. We also asked if the TM motif is essential for SDC1 interaction with ETBP. As predicted, no binding was observed between ETBP and the SDC1-ΔTM truncation mutant (**Figure 4H**). This is also consistent with the previous study that found the TM domain to be essential for ETBP interaction with TPOR [40].

ETBP stabilizes SDC4 and enhances SDC4-associated functions in cancer cells

To further investigate ETBP targeting of SDC4 *in vivo*, we first examined the effect of ETBP on SDC4 protein abundance. Surprisingly, the protein level of SDC4 in PANC1 cells was clearly enhanced upon ETBP treatment (**Figure 5A**). A dose-dependent increase in SDC4 abundance was also observed in the pancreatic cancer cell lines AsPC1 and CFPAC1 with ETBP (**Figure 5B**, **5C**). Given that abnormally up-regulated SDC4 can act as a co-receptor of FGFR to augment the MAPK signaling pathway [10, 12, 38, 41, 42], we further asked whether ETBP could activate MAPK signaling by examining the level of phosphorylated AKT, ERK, and p38. Indeed, ETBP strongly enhanced the phosphorylation of AKT, ERK and p38 in a dose-dependent manner in wild-type PANC1 cells (**Figure 5D**). Importantly, ETBP enhancement of MAPK signaling was significantly attenuated in SDC4 KO cells (Figure S4D).

Considering that SDC4 KO decreased the level of macropinocytosis in PANC1 cells (**Figure 2I**, **2J**), we also asked if ETBP regulated macropinocytosis in pancreatic cancer cells. As illustrated in **Figure 5E-G**, a strong increase in macropinocytosis was detected in all the pancreatic cancer cells examined (PANC1, BxPC3, and AsPC1) with ETBP treatment in a dose dependent manner. Unexpectedly, no clear differences in macropinocytosis were observed between wild-type and SDC4 KO PANC1 cells upon ETBP treatment (Figure S4C), possibly due to the fact that ETBP can target another macropinocytosis mediator SDC1 as well (**Figure 4D**). Taken together, we propose that, similar to ETBP action on its original target TPOR, ETBP is also a potential agonist of SDC4 and enhancer of cancer progression due to its ability to stabilize SDC4, and enhance MAPK signaling as well as macropinocytosis in cancer cells. Caution therefore should be taken when treating cancer patients with ETBP for chemotherapy-induced thrombocytopenia.

Discussion

SDC4 is a transmembrane heparan sulfate proteoglycan that has been extensively connected

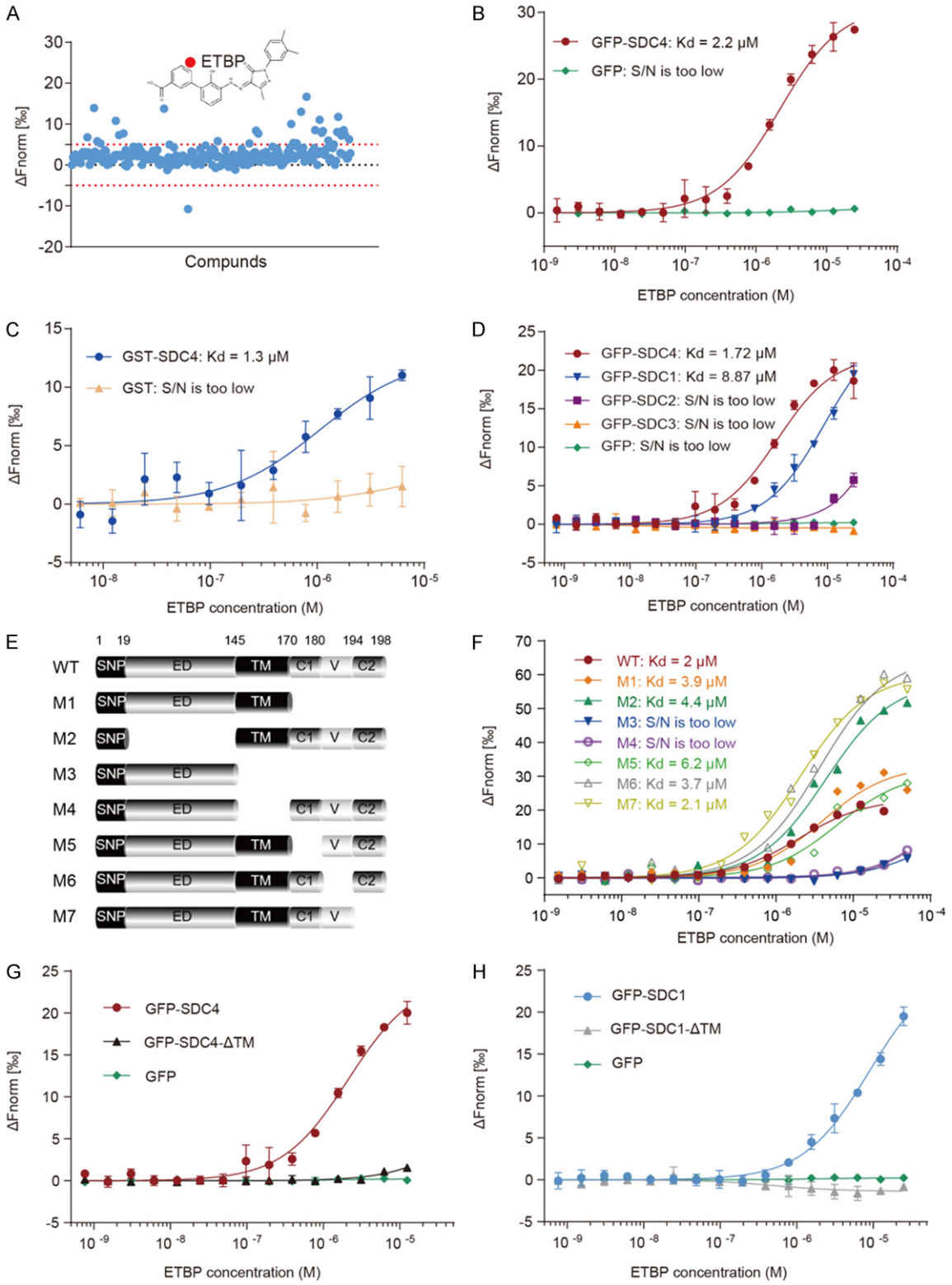

Figure 4. Identification of SDC4-binding agents and the targeting site. (A) A plot of the single-point binding check screening of SDC4-targeting ligands. (B) Microscale Thermophoresis (MST) assays of the interaction between ETBP and GFP-tagged SDC4. ETBP was incubated with HEK293T cell lysate expressing GFP-tagged SDC4 or GFP control, respectively. (C) MST assays of the interaction between ETBP and recombinant GST-tagged SDC4. (D) MST determination of the binding affinity between ETBP and SDC family proteins. (E) Schematic representation of full-length SDC4 and its truncation mutants used in MST assays. The cytoplasmic domain contains two conserved sites C1

and C2 and one variable site V. SNP, signal peptide; ED, extracellular domain; TM, tramsmembrane domain. (F) MST assays for the interaction of ETBP and GFP-tagged SDC4 truncation mutants. (G, H) MST determination of the interaction of ETBP with SDC4-ΔTM (G) or SDC1-ΔTM (H).

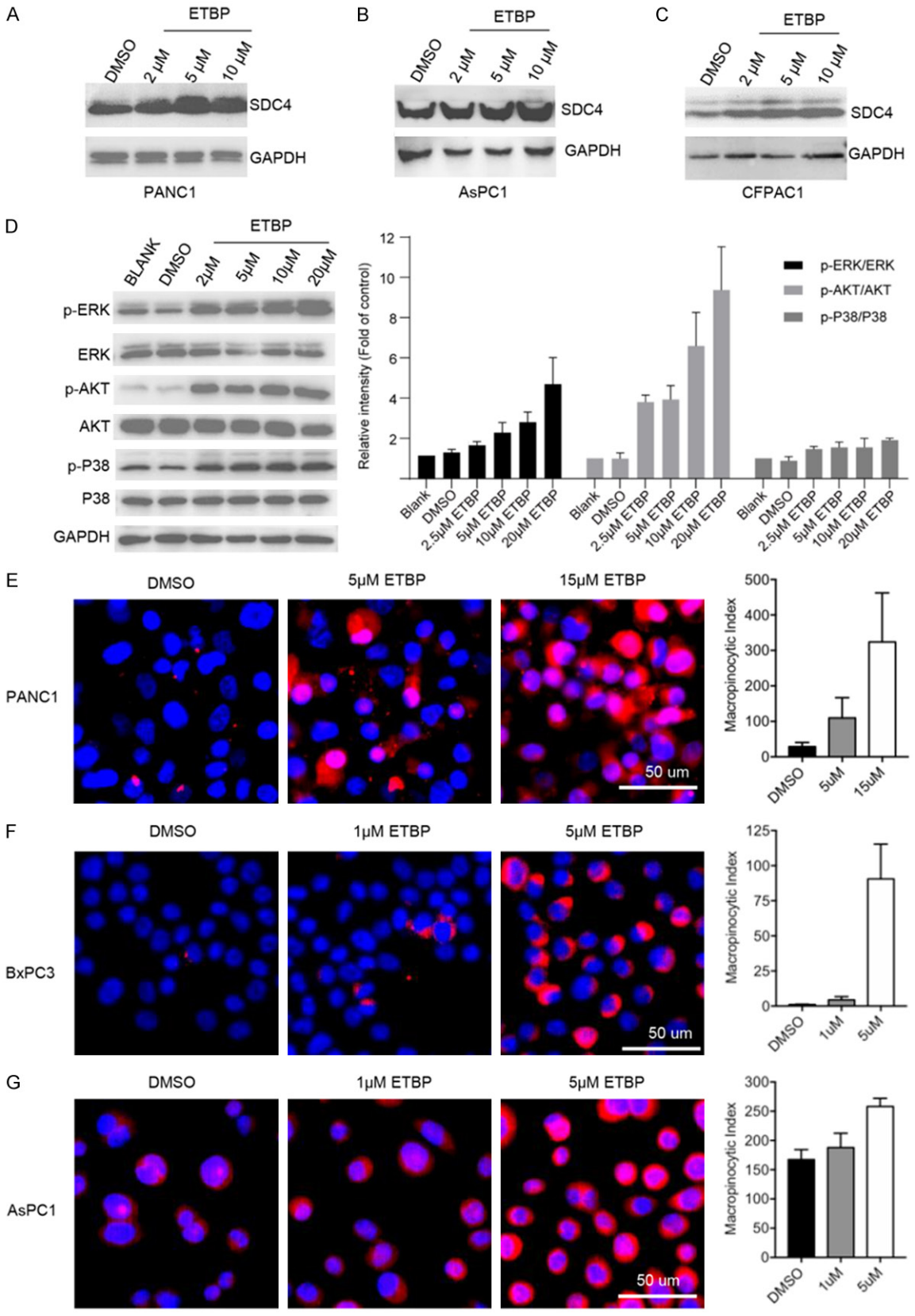

Figure 5. ETBP enhances MAPK signaling pathway and macropinocytosis in cancer cells. (A-C) Western blot assays of SDC4 in PANC1 (A), AsPC1 (B), and CFPAC1 (C) cells treated with ETBP at the indicated concentrations. (D) Western blot assays of phosphorylated and total ERK, AKT, and p38 in PANC1 cells upon ETBP treatment for 12 hours. Quantification analysis of the triplicate experiments is shown. (E-G) Representative macropinocytosis images of PANC1 (E), BxPC3 (F), and AsPC1 (G) cells treated with ETBP at the indicated concentrations. Quantification analysis of macropinocytosis-positive cells is shown. Data are presented as mean ± SD.

with various oncogenic processes [43, 44], although its oncogenic roles were rarely evaluated in loss-of-function assays. In this study, we created SDC4 KO cells using CRISPR/Cas9 and confirmed that *SDC4* deletion in PANC1 cells markedly suppressed the activities of these cells in colony-formation, xenograft initiation and growth, as well as macropinocytosis assays, supporting that SDC4 is a promising target for cancer therapy.

Here we identified a small molecule compound that targets SDC4. SDC4 was previously considered "undruggable" due to its intrinsically disordered structure [21, 22, 45]. Recently, a small molecule bufalin was reported to target SDC4 [10], although it was unclear how the authors discovered this candidate. In the present study, we developed a single-point MST screening assay and identified that ETBP could directly and functionally target the "undruggable" SDC4. Notably, ETBP targets SDC4 at the TM motif, the same region that ETBP binds to with its original target TPOR. Furthermore, we demonstrated that ETBP targeted SDC4 and SDC1 but not SDC2 or SDC3, indicating relative selectivity of ETBP towards SDCs.

An unexpected finding in the present study is that ETBP could positively regulate SDC4. ETBP not only increased the protein level of SDC4, but also enhanced SDC4-dependent MAPK signaling and macropinocytosis in a dose-dependent manner in tumor cells, implying that ETBP is a potential agonist of SDC4. In fact, ETBP was previously identified as a TPOR agonist that could activate STAT5, MARK, and p38 [23]. Of note, we demonstrated that SDC4 was partially required for ETBP activation of MAPK signaling in PANC1 cells (Figure S4D), suggesting that possible synergistic effects between SDC4 and TPOR in ETBP-dependent activation of MAPK signaling.

Given that SDC4 is a positive regulator of cancer cells, we propose that ETBP may be a potential enhancer of cancer progression. We indeed had detected the effect of ETBP on the proliferation of tumor cells. No clear inhibition of ETBP on the colony formation of PANC1 cells was observed up to 10 μM (Figure S4A). Consistently, ETBP did not inhibit cancer proliferation until the dose was increased to 50 μM (Figure S4B). Additionally, at 1 μM and 5 μM, ETBP could slightly promote cell proliferation (Figure S4B), that was consistent with the previous finding that ETBP was capable of inhibiting BAX-mediated apoptosis [46]. As a result, caution should be taken when treating cancer patients with ETBP for chemotherapy-induced thrombocytopenia [27].

Acknowledgements

This work was supported by the Natural Science Foundation of China (31800668, 81703757, 81874210, 81874319), the Science and Technology Commission of Shanghai Municipality (18401933500, 21S11900900), Shanghai Municipal Education Commission (2019-01-07-00-10-E00072, 2021-01-07-00-10-E00116), Shanghai Youth Talent Support Program, Shuguang Project (19SG40), and the Program for Professor of Special Appointment (Eastern Scholar).

Disclosure of conflict of interest

None.

Address correspondence to: Xisong Ke, Xianglian Zhou and Yi Qu, Center for Chemical Biology, Institute of Interdisciplinary Integrative Medicine Research, Shanghai University of Traditional Chinese Medicine, Shanghai, China. E-mail: xisongke@shutcm.edu.cn (XSK); zhouxianglian@shutcm.edu.cn (XLZ); yiqu@shutcm.edu.cn (YQ)

References

[1] Agere SA, Kim EY, Akhtar N and Ahmed S. Syndecans in chronic inflammatory and autoimmune diseases: pathological insights and therapeutic opportunities. J Cell Physiol 2018; 233: 6346-6358.

[2] Betriu N, Bertran-Mas J, Andreeva A and Semino CE. Syndecans and pancreatic ductal adenocarcinoma. Biomolecules 2021; 11: 349.
[3] Gondelaud F and Ricard-Blum S. Structures and interactions of syndecans. FEBS J 2019; 286: 2994-3007.
[4] Ibrahim SA, Gadalla R, El-Ghonaimy EA, Samir O, Mohamed HT, Hassan H, Greve B, El-Shinawi M, Mohamed MM and Götte M. Syndecan-1 is a novel molecular marker for triple negative inflammatory breast cancer and modulates the cancer stem cell phenotype via the IL-6/STAT3, Notch and EGFR signaling pathways. Mol Cancer 2017; 16: 57.
[5] Popović A, Demirović A, Spajić B, Stimac G, Kruslin B and Tomas D. Expression and prognostic role of syndecan-2 in prostate cancer. Prostate Cancer Prostatic Dis 2010; 13: 78-82.
[6] Han YD, Oh TJ, Chung TH, Jang HW, Kim YN, An S and Kim NK. Early detection of colorectal cancer based on presence of methylated syndecan-2 (SDC2) in stool DNA. Clin Epigenetics 2019; 11: 51.
[7] Yao W, Rose JL, Wang W, Seth S, Jiang H, Taguchi A, Liu J, Yan L, Kapoor A, Hou P, Chen Z, Wang Q, Nezi L, Xu Z, Yao J, Hu B, Pettazzoni PF, Ho IL, Feng N, Ramamoorthy V, Jiang S, Deng P, Ma GJ, Den P, Tan Z, Zhang SX, Wang H, Wang YA, Deem AK, Fleming JB, Carugo A, Heffernan TP, Maitra A, Viale A, Ying H, Hanash S, DePinho RA and Draetta GF. Syndecan 1 is a critical mediator of macropinocytosis in pancreatic cancer. Nature 2019; 568: 410-414.
[8] Jechorek D, Haeusler-Pliske I, Meyer F and Roessner A. Diagnostic value of syndecan-4 protein expression in colorectal cancer. Pathol Res Pract 2021; 222: 153431.
[9] Onyeisi JOS, Lopes CC and Götte M. Syndecan-4 as a pathogenesis factor and therapeutic target in cancer. Biomolecules 2021; 11: 503.
[10] Yang H, Liu Y, Zhao MM, Guo Q, Zheng XK, Liu D, Zeng KW and Tu PF. Therapeutic potential of targeting membrane-spanning proteoglycan SDC4 in hepatocellular carcinoma. Cell Death Dis 2021; 12: 492.
[11] Keller-Pinter A, Gyulai-Nagy S, Becsky D, Dux L and Rovo L. Syndecan-4 in tumor cell motility. Cancers (Basel) 2021; 13: 3322.
[12] Forsten-Williams K, Chua CC and Nugent MA. The kinetics of FGF-2 binding to heparan sulfate proteoglycans and MAP kinase signaling. J Theor Biol 2005; 233: 483-499.
[13] Leonova EI and Galzitskaya OV. Structure and functions of syndecans in vertebrates. Biochemistry (Mosc) 2013; 78: 1071-1085.
[14] Fitzgerald ML, Wang Z, Park PW, Murphy G and Bernfield M. Shedding of syndecan-1 and -4 ectodomains is regulated by multiple signaling pathways and mediated by a TIMP-3-sensitive metalloproteinase. J Cell Biol 2000; 148: 811-824.
[15] Reine TM, Lanzalaco F, Kristiansen O, Enget AR, Satchell S, Jenssen TG and Kolset SO. Matrix metalloproteinase-9 mediated shedding of syndecan-4 in glomerular endothelial cells. Microcirculation 2019; e12534.
[16] Bollmann M, Pinno K, Ehnold LI, Märtens N, Märtson A, Pap T, Stärke C, Lohmann CH and Bertrand J. MMP-9 mediated Syndecan-4 shedding correlates with osteoarthritis severity. Osteoarthritis Cartilage 2021; 29: 280-289.
[17] Manon-Jensen T, Itoh Y and Couchman JR. Proteoglycans in health and disease: the multiple roles of syndecan shedding. FEBS J 2010; 277: 3876-3889.
[18] Choi S, Lee H, Choi JR and Oh ES. Shedding; towards a new paradigm of syndecan function in cancer. BMB Rep 2010; 43: 305-310.
[19] Rangarajan S, Richter JR, Richter RP, Bandari SK, Tripathi K, Vlodavsky I and Sanderson RD. Heparanase-enhanced shedding of syndecan-1 and its role in driving disease pathogenesis and progression. J Histochem Cytochem 2020; 68: 823-840.
[20] Peysselon F, Xue B, Uversky VN and Ricard-Blum S. Intrinsic disorder of the extracellular matrix. Mol Biosyst 2011; 7: 3353-3365.
[21] Leonova EI and Galzitskaya OV. Cell communication using intrinsically disordered proteins: what can syndecans say? J Biomol Struct Dyn 2015; 33: 1037-1050.
[22] Santos R, Ursu O, Gaulton A, Bento AP, Donadi RS, Bologa CG, Karlsson A, Al-Lazikani B, Hersey A, Oprea TI and Overington JP. A comprehensive map of molecular drug targets. Nat Rev Drug Discov 2017; 16: 19-34.
[23] Erickson-Miller CL, DeLorme E, Tian SS, Hopson CB, Stark K, Giampa L, Valoret EI, Duffy KJ, Luengo JL, Rosen J, Miller SG, Dillon SB and Lamb P. Discovery and characterization of a selective, nonpeptidyl thrombopoietin receptor agonist. Exp Hematol 2005; 33: 85-93.
[24] Bussel J, Kulasekararaj A, Cooper N, Verma A, Steidl U, Semple JW and Will B. Mechanisms and therapeutic prospects of thrombopoietin receptor agonists. Semin Hematol 2019; 56: 262-278.
[25] Ghanima W, Cooper N, Rodeghiero F, Godeau B and Bussel JB. Thrombopoietin receptor agonists: ten years later. Haematologica 2019; 104: 1112-1123.
[26] Townsley DM, Scheinberg P, Winkler T, Desmond R, Dumitriu B, Rios O, Weinstein B, Valdez J, Lotter J, Feng X, Desierto M, Leuva H, Bevans M, Wu C, Larochelle A, Calvo KR, Dunbar CE and Young NS. Eltrombopag added to

standard immunosuppression for aplastic anemia. N Engl J Med 2017; 376: 1540-1550.
[27] Zhang X, Chuai Y, Nie W, Wang A and Dai G. Thrombopoietin receptor agonists for prevention and treatment of chemotherapy-induced thrombocytopenia in patients with solid tumours. Cochrane Database Syst Rev 2017; 11: CD012035.
[28] Ballmaier M and Germeshausen M. Advances in the understanding of congenital amegakaryocytic thrombocytopenia. Br J Haematol 2009; 146: 3-16.
[29] Kapoor S, Champion G and Olnes MJ. Thrombopoietin receptor agonists for marrow failure: a concise clinical review. Best Pract Res Clin Haematol 2021; 34: 101274.
[30] Schmitt N, Jann JC, Altrock E, Flach J, Danner J, Uhlig S, Streuer A, Knaflic A, Riabov V, Xu Q, Mehralivand A, Palme I, Nowak V, Obländer J, Weimer N, Haselmann V, Jawhar A, Darwich A, Weis CA, Marx A, Steiner L, Jawhar M, Metzgeroth G, Boch T, Nolte F, Hofmann WK and Nowak D. Preclinical evaluation of eltrombopag in a PDX model of myelodysplastic syndromes. Leukemia 2021; 36: 236-247.
[31] Baba F, Swartz K, van Buren R, Eickhoff J, Zhang Y, Wolberg W and Friedl A. Syndecan-1 and syndecan-4 are overexpressed in an estrogen receptor-negative, highly proliferative breast carcinoma subtype. Breast Cancer Res Treat 2006; 98: 91-98.
[32] O'Connell MP, Fiori JL, Kershner EK, Frank BP, Indig FE, Taub DD, Hoek KS and Weeraratna AT. Heparan sulfate proteoglycan modulation of Wnt5A signal transduction in metastatic melanoma cells. J Biol Chem 2009; 284: 28704-28712.
[33] Erdem M, Erdem S, Sanli O, Sak H, Kilicaslan I, Sahin F and Telci D. Up-regulation of TGM2 with ITGB1 and SDC4 is important in the development and metastasis of renal cell carcinoma. Urol Oncol 2014; 32: 25.
[34] Baietti MF, Zhang Z, Mortier E, Melchior A, Degeest G, Geeraerts A, Ivarsson Y, Depoortere F, Coomans C, Vermeiren E, Zimmermann P and David G. Syndecan-syntenin-ALIX regulates the biogenesis of exosomes. Nat Cell Biol 2012; 14: 677-685.
[35] Roucourt B, Meeussen S, Bao J, Zimmermann P and David G. Heparanase activates the syndecan-syntenin-ALIX exosome pathway. Cell Res 2015; 25: 412-428.
[36] Ghossoub R, Chéry M, Audebert S, Leblanc R, Egea-Jimenez AL, Lembo F, Mammar S, Le Dez F, Camoin L, Borg JP, Rubinstein E, David G and Zimmermann P. Tetraspanin-6 negatively regulates exosome production. Proc Natl Acad Sci U S A 2020; 117: 5913-5922.
[37] Nakase I, Osaki K, Tanaka G, Utani A and Futaki S. Molecular interplays involved in the cellular uptake of octaarginine on cell surfaces and the importance of syndecan-4 cytoplasmic V domain for the activation of protein kinase Cα. Biochem Biophys Res Commun 2014; 446: 857-862.
[38] Elfenbein A and Simons M. Syndecan-4 signaling at a glance. J Cell Sci 2013; 126: 3799-3804.
[39] Qu Y, Gharbi N, Yuan X, Olsen JR, Blicher P, Dalhus B, Brokstad KA, Lin B, Øyan AM, Zhang W, Kalland KH and Ke X. Axitinib blocks Wnt/β-catenin signaling and directs asymmetric cell division in cancer. Proc Natl Acad Sci U S A 2016; 113: 9339-9344.
[40] Kim MJ, Park SH, Opella SJ, Marsilje TH, Michellys PY, Seidel HM and Tian SS. NMR structural studies of interactions of a small, nonpeptidyl Tpo mimic with the thrombopoietin receptor extracellular juxtamembrane and transmembrane domains. J Biol Chem 2007; 282: 14253-14261.
[41] Echtermeyer F, Bertrand J, Dreier R, Meinecke I, Neugebauer K, Fuerst M, Lee YJ, Song YW, Herzog C, Theilmeier G and Pap T. Syndecan-4 regulates ADAMTS-5 activation and cartilage breakdown in osteoarthritis. Nat Med 2009; 15: 1072-1076.
[42] Choi S, Lee E, Kwon S, Park H, Yi JY, Kim S, Han IO, Yun Y and Oh ES. Transmembrane domain-induced oligomerization is crucial for the functions of syndecan-2 and syndecan-4. J Biol Chem 2005; 280: 42573-42579.
[43] Tkachenko E, Rhodes JM and Simons M. Syndecans: new kids on the signaling block. Circ Res 2005; 96: 488-500.
[44] Afratis NA, Nikitovic D, Multhaupt HA, Theocharis AD, Couchman JR and Karamanos NK. Syndecans - key regulators of cell signaling and biological functions. FEBS J 2017; 284: 27-41.
[45] Cruz-Chu ER, Malafeev A, Pajarskas T, Pivkin IV and Koumoutsakos P. Structure and response to flow of the glycocalyx layer. Biophys J 2014; 106: 232-243.
[46] Spitz AZ, Zacharioudakis E, Reyna DE, Garner TP and Gavathiotis E. Eltrombopag directly inhibits BAX and prevents cell death. Nat Commun 2021; 12: 1134.
[47] Commisso C, Flinn RJ and Bar-Sagi D. Determining the macropinocytic index of cells through a quantitative image-based assay. Nat Protoc 2014; 9: 182-192.
[48] Franken NA, Rodermond HM, Stap J, Haveman J and van Bree C. Clonogenic assay of cells in vitro. Nat Protoc 2006; 1: 2315-2319.

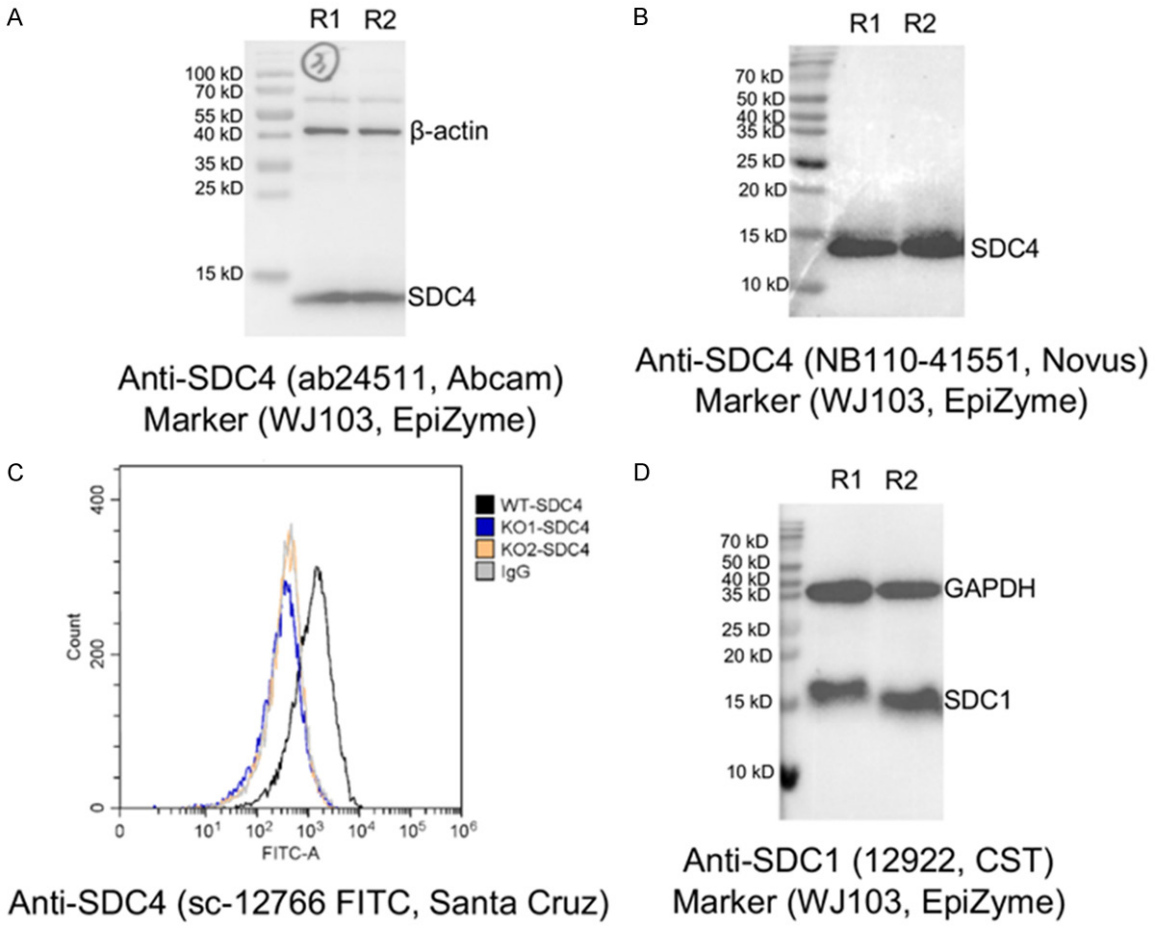

Figure S1. Related to **Figure 1**. Confirmation of Western Blot bands of SDC4 and SDC1. A. Western blot of SDC4 by Abcam antibody using PANC1 cell lysate. B. Western blot of SDC4 by Novus antibody using PANC1 cell lysate. C. Surface expression of SDC4 was measured by flow cytometry to confirm SDC4 depletion using Santa Cruz antibody; representative histograms are shown. Experiments were repeated twice with similar results. D. Western blot of SDC1 by CST antibody using PANC1 cell lysate. R1, represention 1; R2, represention 2.

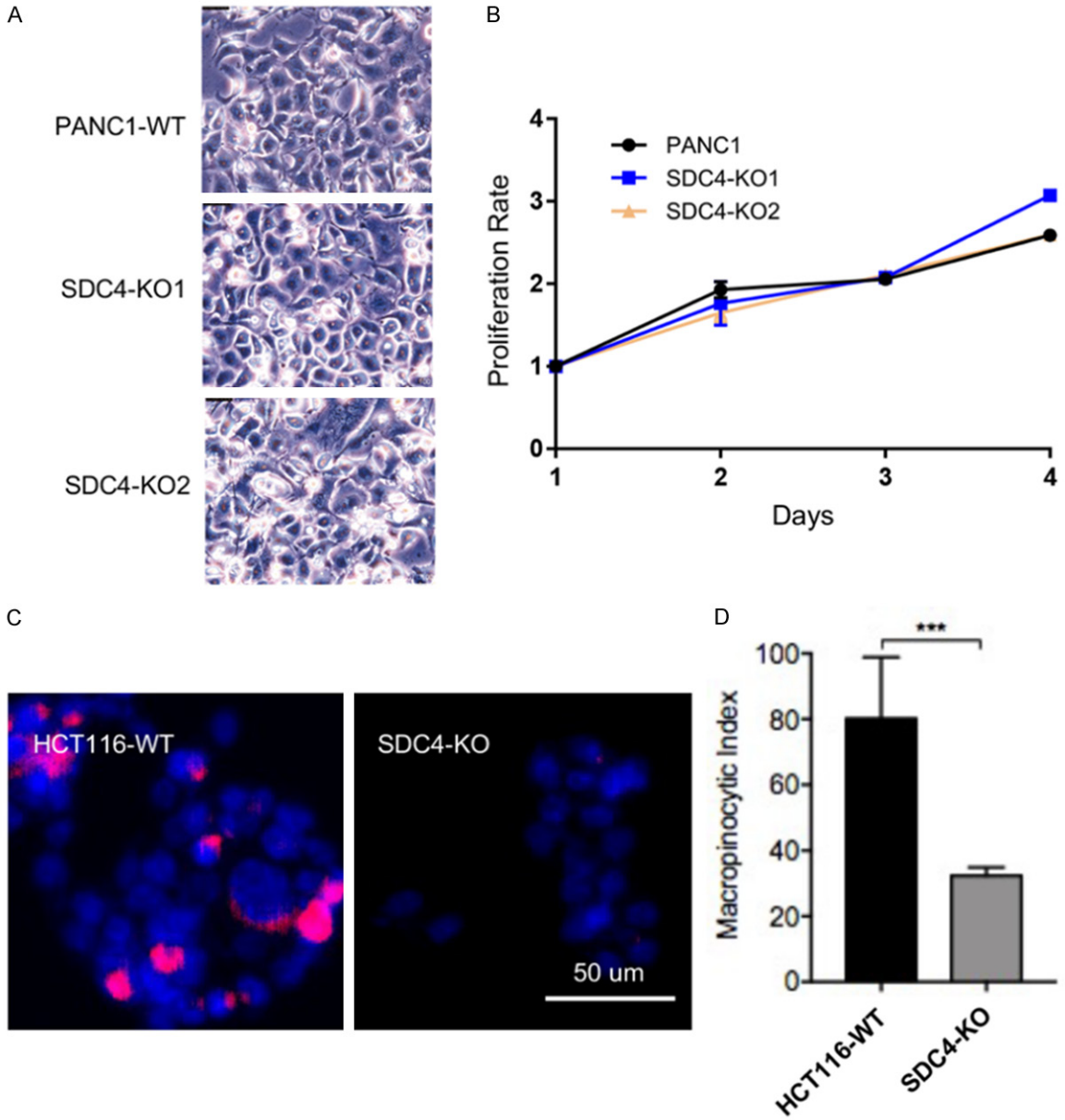

Figure S2. Related to **Figure 2**. The phenotype of SDC4 knock out cells. The epithelial morphology (A) and growth rate comparison (B) of PANC1 wild-type and SDC4 knockout cells. Macropinocytosis was visualized with TMR-dextran (scale bar, 50 μm) (C) and quantified (D), data are mean ± s.d. in HCT116 wide-type and SDC4 knockout cells.

Table S1. The 89 differentially expressed proteins identified from SDC4 KO PANC1 cells by proteomic profiling analysis

Gene names	LFQ intensity					
	PANC1-WT-1	PANC1-WT-2	PANC1-SDC4-KO1-1	PANC1-SDC4-KO1-2	PANC1-SDC4-KO2-1	PANC1-SDC4-KO2-2
ABCB6	10736000	9641700	0	0	0	0
ABHD14B	1381300000	1384100000	796090000	816930000	907200000	856730000
ACAD9	628410000	604490000	982400000	1053700000	1044900000	1103300000
ACADVL	2868300000	2882500000	1614600000	1729600000	1602700000	1582600000
AIFM2	121220000	130360000	68960000	77747000	57058000	63976000
AKAP12	8362600000	8479800000	4076100000	4094200000	4022500000	4040100000
ALPP	15773000	15623000	0	0	0	0
ALPPL2	389340000	393540000	101190000	66160000	36912000	58669000
ANXA3	35562000	34441000	20203000	22364000	251750000	244760000
ANXA7	1907800000	1797800000	3000300000	2881400000	3179200000	3089800000
APP	569060000	554730000	297450000	295520000	320350000	331160000
ARRB1	1557000000	1565000000	904920000	969130000	932580000	860240000
BCAS1	0	0	24961000	21536000	23270000	24796000
BEND3	12838000	13138000	0	0	0	0
C16orf13	4952800	5372500	0	0	0	0
CAPG	4640300000	4656800000	2272200000	2259500000	2720000000	2751100000
CBR1	705210000	733120000	391480000	379860000	428110000	458480000
CBS	901960000	894670000	459240000	446260000	569240000	539350000
CDCP1	481040000	453780000	225620000	240890000	307090000	269300000
CKB	1238900000	1284500000	2546500000	2466200000	2442500000	2576000000
COL16A1	8786000	8589300	0	0	0	0
COL18A1	1748400000	1673600000	862690000	907310000	638300000	624760000
COPG2	452900000	463640000	707170000	698040000	690390000	698280000
CSNK1E	8594500	9545900	4622300	4983500	0	0
CTSC	716750000	669410000	217620000	209840000	254480000	268500000
DGAT1	97900000	106730000	69966000	57302000	72653000	60505000
DIS3L2	155270000	151630000	74316000	85769000	78773000	64448000
DNAJB12	173000000	160080000	284210000	285710000	286880000	274970000
ECHDC1	486130000	469020000	279430000	276750000	257970000	258030000
EIF4B	4871400000	5301200000	3364400000	3198000000	2902200000	2542200000
ENO3	28743000	27863000	0	3697400	0	0
FBXO2	596890000	628590000	1019900000	1091600000	990460000	957410000
FOXS1; FOXC2; FOXC1	11925000	12864000	0	0	0	0
GCA	60991000	63492000	219530000	201200000	143450000	140210000
GJA1	69313000	64860000	125750000	122110000	163890000	163830000
GPX1	164650000	154110000	82219000	78329000	105730000	87550000
H1F0	384890000	405980000	206020000	176860000	195090000	206810000
ICAM1	665020000	605940000	1679800000	1749000000	1784500000	1821200000
ISYNA1	588300000	609630000	350510000	307760000	288870000	321960000
ITGA2	1762300000	1716000000	634520000	620630000	1045000000	1149300000
KDELR1; KDELR2	48007000	54632000	22489000	26568000	9989900	12828000
KRT1	3650900000	3144600000	302690000	398580000	940580000	587230000
MAP2	187320000	152110000	1150000000	1070600000	294620000	264460000
MEGF6	1162300	1666600	2906700	3262400	4022700	3562900
MISP	412740000	401730000	193710000	218330000	250260000	269390000
MTERF3	104130000	90583000	147280000	155990000	149290000	168470000
MTHFD1L	916350000	967870000	585120000	589390000	624440000	612690000

MYH10	683020000	703130000	1195400000	1228000000	267970000	257270000
MYL6B	14341000	13641000	0	0	0	0
MYPN	689170000	667340000	1226100000	1250500000	2119600000	1927300000
NAMPT	2003400000	2057800000	3569200000	3532900000	3407100000	3334800000
NAPRT	122410000	138480000	34425000	31769000	29896000	24533000
NCKIPSD	33028000	29171000	13912000	8958100	16017000	12902000
NEU1	216990000	203320000	452070000	409610000	564610000	557660000
NMES1; C15orf48	783090000	756630000	2045900000	2190600000	1974600000	2017800000
PAK2	3818900000	3688600000	6140400000	6628200000	6140500000	5966600000
PARG	250440000	230120000	375210000	416600000	360790000	378430000
PCYT1A	616050000	641760000	1065800000	1088800000	1116800000	1034900000
PFKM	492320000	488760000	302550000	282490000	268140000	253080000
PKP3	228670000	239280000	77481000	94267000	147380000	124520000
PLXNA1	39142000	54447000	131020000	150950000	138550000	143890000
PODXL	308200000	341620000	531580000	510800000	491720000	526770000
POR	873930000	793980000	1301500000	1231500000	1440700000	1331600000
PRDX2	1303400000	1308900000	176480000	185040000	403410000	426060000
QPRT	11214000	10064000	3313800	3971100	0	0
RAB6B	33403000	32355000	59506000	64269000	65169000	61853000
RNASET2	32716000	31310000	0	0	19681000	17219000
SCARB1	99541000	116660000	168500000	190180000	167550000	180350000
SCRN1	1355300000	1373900000	2244100000	2206600000	2034000000	2081700000
SDSL	52299000	51240000	23194000	21686000	27699000	31100000
SEC24C	1662200000	1742100000	2903700000	2954600000	3277800000	3149800000
SF1	2612300000	2625100000	2898600000	2662200000	2438200000	2588800000
SLC12A2	513070000	523240000	297150000	317630000	288170000	283590000
SNCA	123600000	137600000	17051000	18627000	0	15186000
SNCG	5252000	5561900	0	0	0	0
SQSTM1	3085700000	3081900000	5689000000	5531500000	7719800000	7662800000
STMN2	676360000	603910000	292200000	249800000	88618000	92150000
SYT1	23699000	26256000	0	0	0	0
TFG	1305000000	1260400000	2291300000	2332800000	2225700000	2220000000
TFRC	2454200000	2503000000	4641200000	4996500000	4306200000	4260400000
TMEM65	139730000	151060000	65746000	74883000	75946000	86608000
TMUB2	50980000	56302000	85962000	88971000	97218000	93467000
TP53I11	157360000	163600000	252910000	243680000	288530000	301800000
TRIM44	9585800	10844000	0	0	18299000	16272000
TSC22D4	116210000	113850000	213150000	226260000	192650000	199270000
UBE2J1	15324000	13827000	24142000	22418000	23438000	22659000
UGDH	8559900000	8333600000	13386000000	13452000000	12493000000	13060000000
VCL	21093000000	20595000000	44588000000	44272000000	49223000000	48206000000
VDAC2	5230800000	5076400000	8391300000	8295900000	8083900000	7564300000

The proteins with change fold over 1.5 were filtered. Each sample was repeated twice. T-test was performed to identify significantly changed proteins. Totally 89 proteins were consistently changed in both SDC4 knockout cell clones.

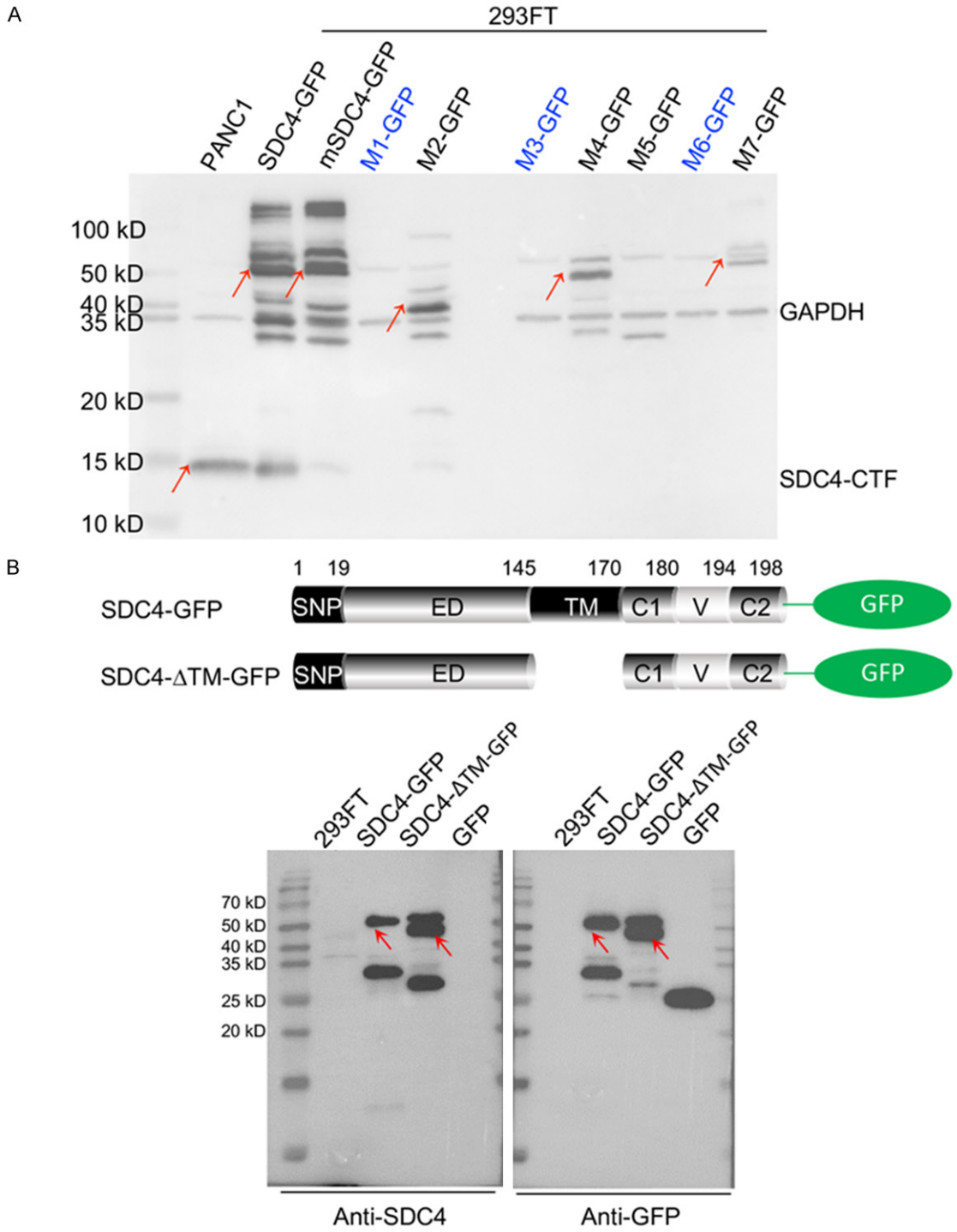
A
293FT
PANC1
SDC4-GFP
mSDC4-GFP
M1-GFP
M2-GFP
M3-GFP
M4-GFP
M5-GFP
M6-GFP
M7-GFP
100 kD
50 kD
40 kD
35 kD
20 kD
15 kD
10 kD
GAPDH
SDC4-CTF
B
1
19
145
170
180
194
198
SDC4-GFP
SNP
ED
TM
C1
V
C2
GFP
SDC4-ΔTM-GFP
SNP
ED
C1
V
C2
GFP
293FT
SDC4-GFP
SDC4-ΔTM-GFP
GFP
293FT
SDC4-GFP
SDC4-ΔTM-GFP
GFP
70 kD
50 kD
40 kD
35 kD
25 kD
20 kD
Anti-SDC4
Anti-GFP

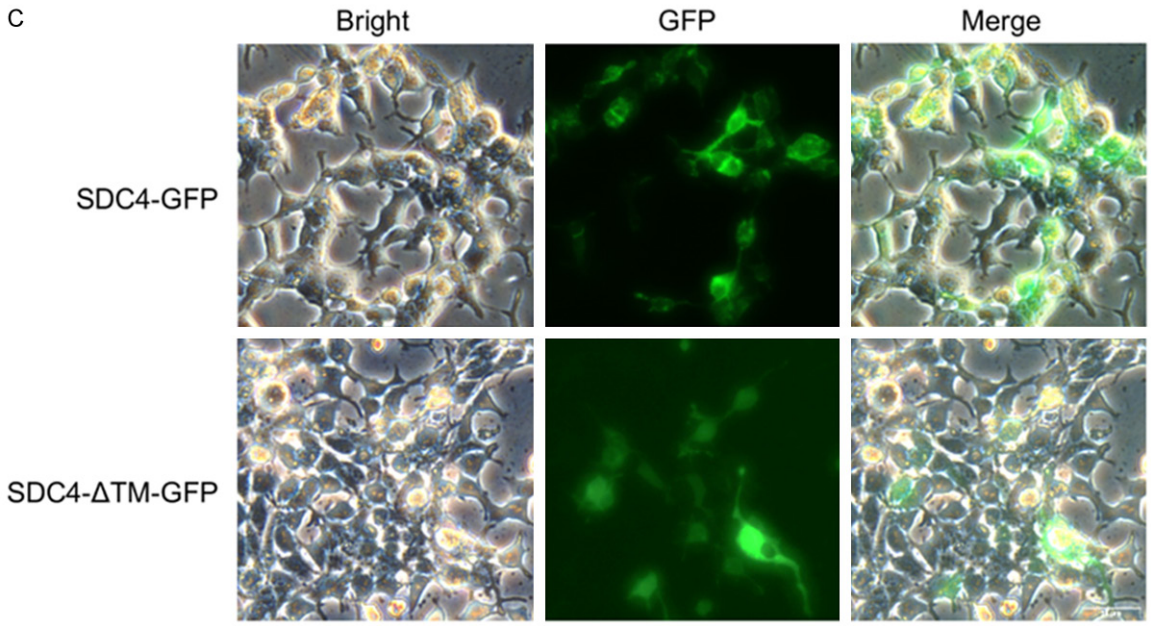

Figure S3. Related to **Figure 4**. Western Blot of SDC4 truncations used in MST assay. A. Western blot of GFP fused SDC4 truncations used in **Figure 4F**. B. Western blot of GFP fused SDC4 and SDC4-ΔTM used in **Figure 4G**. C. Images of GFP fluorescence by overexpressed SDC4 and SDC4-ΔTM in 293 cells.

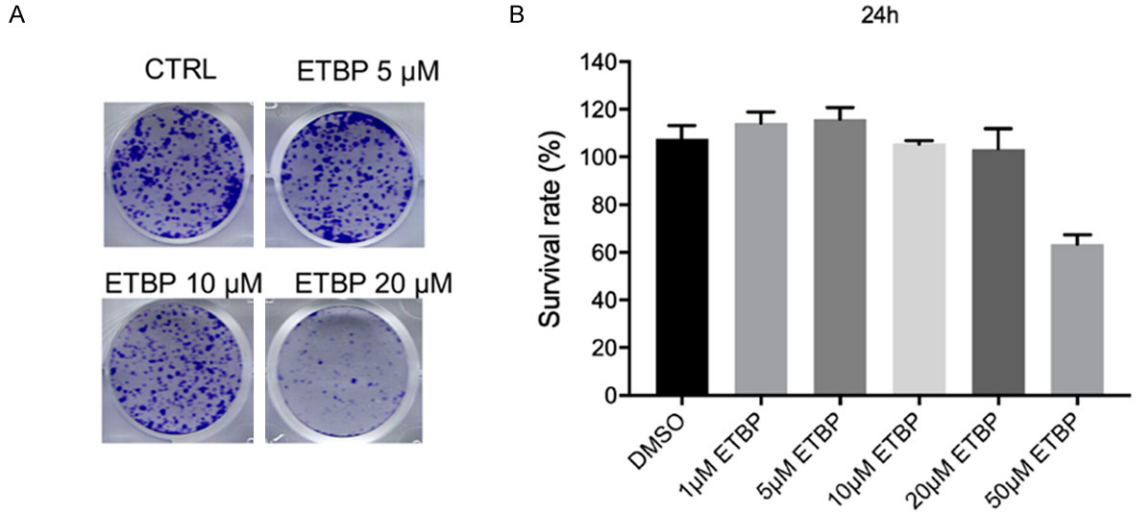

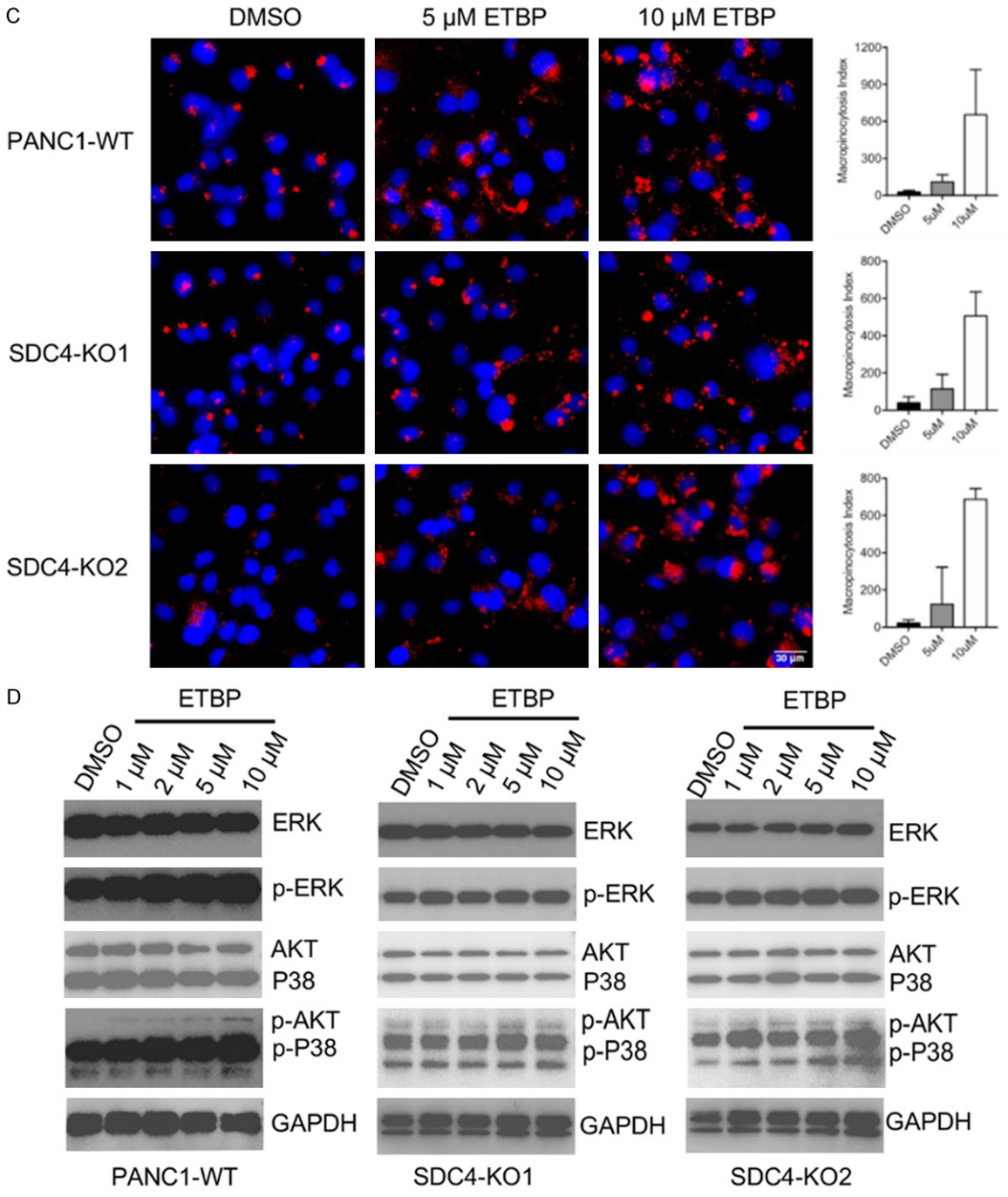

Figure S4. Related to **Figure 5**. The effects of ETBP on SDC4 knockout PANC1 cells. A. The result of Colony-formation assay of PANC1 cells treated with ETBP at the indicated concentrations for 14 days. B. The result of CCK8 assay of PANC1 cells treated with ETBP for 24 hours. Experiments were performed in triplicates. C. Representative images of Macropinocytosis treated with the indicated concentration of ETBP in wild-type and SDC4 knockout PANC1 cells, and statistical analysis. D. Non-phosphorylations/phosphorylations of ERK, AKT, and P38 were detected by western blot after 12 h incubation with the indicated concentration of ETBP in wild-type and SDC4 knockout PANC1 cells respectively.